PROTEINS
STRUCTURE ■ FUNCTION ■ BIOINFORMATICS

Crystal structure of glycerophosphodiester phosphodiesterase (GDPD) from *Thermoanaerobacter tengcongensis*, a metal ion-dependent enzyme: Insight into the catalytic mechanism

Liang Shi, Jun-Feng Liu, Xiao-Min An, and Dong-Cai Liang*

National Laboratory of Biomacromolecules, Institute of Biophysics, Chinese Academy of Sciences, Beijing 100101, People's Republic of China

ABSTRACT

Glycerophosphodiester phosphodiesterase (GDPD; EC 3.1.4.46) catalyzes the hydrolysis of a glycerophosphodiester to an alcohol and glycerol 3-phosphate in glycerol metabolism. It has an important role in the synthesis of a variety of products that participate in many biochemical pathways. We report the crystal structure of the Thermoanaerobacter tengcongensis GDPD (ttGDPD) at 1.91 Å resolution, with a calcium ion and glycerol as a substrate mimic coordinated at this calcium ion (PDB entry 2pz0). The ttGDPD dimer with an intermolecular disulfide bridge and two hydrogen bonds is considered as the potential functional unit. We used site-directed mutagenesis to characterize ttGDPD as a metal ion-dependent enzyme, identified a cluster of residues involved in substrate binding and the catalytic reaction, and we propose a possible general acid-base catalytic mechanism for ttGDPD. Superposing the active site with the homologous structure GDPD from Agrobacterium tumefaciens (PDB entry 1zcc), which binds a sulfate ion in the active site, the sulfate ion can represent the phosphate moiety of the substrate, simulating the binding mode of the true substrate of GDPD.

Proteins 2008; 72:280–288.

Key words: *crystal structure; glycerophosphodiester phosphodiesterase; Thermo anaerobacter tengcongensis; metal ion-dependent enzyme; catalytic mechanism.*

INTRODUCTION

The role of glycerophosphodiester phosphodiesterase (GDPD; EC 3.1.4.46) is to hydrolyze deacylated phospholipids to an alcohol and glycerol 3-phosphate (G3P)[1]:

$$\text{glycerophosphodiester} + H_2O \rightarrow \text{an alcohol} + \textit{sn}\text{-glycerol 3-phosphate}$$

Bacteria, archea and eukaryotes,[2–4] and higher mammals including human[5] have GDPD. The enzyme was first identified in *Escherichia coli* and showed specificity for a variety of glycerophosphodiesters, such as glycerophosphocholine, glycerophosphoethanolamine, glycerophosphoglycerol, and bis(glycerophosphoglycerol).[1] In prokaryotes, GDPD is a periplasmic protein that provides cells with the necessary glycerol 3-P,[6] by hydrolysis of glycerophosphodiesters, to participate in the glycerol and glycerol 3-P metabolism.[1,7] Some pathogens, such as *Haemophilus influenzae*, can use GDPD to hydrolyze abundant phosphatidylcholine from host membranes to obtain free choline on the lipopolysaccharides on the bacteria surface that contribute the pathogenesis.[8] In eukaryotes, membrane proteins that contain the GDPD motif, with GDPD activity, form a large family with roles in phospholipid metabolism, cytoskeletal modification, motor neuron differentiation, and as a virulence factor.[4,9,10]

To date, several structures of GDPD from prokaryotes have been solved; the first GDPD structure was from *Thermotoga maritime*,[11] and a cluster of conserved residues were identified in this structure. Because of the lack of bound ligand, the groove surrounded by these residues can only be suggested to be the active region. The GDPD structure from *Agrobacterium tumefaciens* has a sulfate ion and an acetate ion located at that groove,[12] but no more information about the catalytic mechanism of GDPD is

Abbreviations: CATH, a hierarchical classification of protein domain structures, which clusters proteins at four major levels, Class(C), Architecture(A), Topology(T) and Homologous superfamily (H); GDPD, glycerophosphodiester phosphodiesterase; PDB, Protein Data Bank; PI-PLC, phosphatidylinositol-specific phospholipase C; r.m.s.d., root mean square deviation; TIM, triose-phosphate isomerase.

Grant sponsors: National Basic Research Program (973, No. 2002CB713801 and 2006CB806501), National Protein Project (No. 2006CB910902).
*Correspondence to: Dong-Cai Liang, National Laboratory of Biomacromolecules, Institute of Biophysics, CAS, 15 Datun Road, Chaoyang District, Beijing 100101, China. E-mail: dcliang@sun5.ibp.ac.cn
Received 30 August 2007; Revised 31 October 2007; Accepted 8 November 2007
Published online 23 January 2008 in Wiley InterScience (www.interscience.wiley.com).
DOI: 10.1002/prot.21921

available. Recently, a crystal structure of GDPD from *Enterobacter aerogenes* has been reported that allows discussion of the mechanism of GDPD action.[13,14] In some other homologous structures available in the Protein Data Bank (1T8Q, 1YDY, and 2OOG), a Ca atom or some similar metal ion (Mg, Zn, etc.) is found at the active site, and several of those structures bind glycerol at the metal ion, but the catalytic mechanism of GDPD is not clear. In addition, a molecule 3D model of GDPD from mammalian, GDE1, has been generated by bioinformatics[15] and predicted some features about key residues of GDPDs.

We report the crystal structure of GDPD from *Thermoanaerobobacters tengcongensis* (ttGDD)[16] with a Ca atom chelated by three conserved residues (E44, D46, and E119), and a glycerol molecule bound at it in that groove. The results of multisequence alignment and comparison of structures of ttGDPD with the homologous structures from other species reveal strict conservation of some residues.

To elucidate the catalytic mechanism, we used site-directed mutagenesis to make a series of converted residues. We have characterized for the first time ttGDPD as a metal ion-dependent enzyme. On the basis of the catalytic mechanism of PI-PLC, an enzyme that catalyzes the similar hydrolysis of the 3′-5′ phosphodiester bond,[17] we have identified the residues participating in the catalysis, and we propose the catalytic mechanism of ttGDPD. There is a sulfate ion in the active site of homologous structure GDPD from *A. tumefaciens* (PDB entry 1zcc),[12] which is equivalent to the phosphate moiety of the substrate, allowing us to study the true substrate-binding mode of ttGDPD.

Table I
Data Collection Statistics and Refinement Statistics

Data collection statistics	
Space group	$P2_1$
Unit cell parameters	
a (Å)	49.401
b (Å)	53.608
c (Å)	110.885
β (°)	97.911
Resolution (Å)	50–1.91
No. reflections	218,286
No. unique reflections	44,716
Redundancy	4.88
R_{merge} (%)	5.2 (32.2)
Completeness (%)	99.6 (98.8)
I/σ (I)	25 (4.5)
No. monomers per asymmetric unit	2
Refinement statistics	
Resolution (Å)	10–1.91
R_{work} (%)	22.9
R_{free} (%)	23.6
r.m.s.d. from ideal	
Bonds length (Å)	0.0098
Bond angles (°)	1.16
Mean *B*-factor (Å^2)	28.27
Ramachandran plot	
Most favored regions (%)	92.0
Allowed regions (%)	7.8
Generously allowed regions (%)	0.2
Disallowed regions (%)	0

EXPERIMENTAL PROCEDURES

Gene clone and site-directed mutagenesis

The full length of the gene encoding ttGDPD was amplified by PCR from *T. tengcongensis* genomic DNA.[18] The product of PCR was subcloned into the pETM-10 vector using the restriction sites of *Nco*I and *Hind*III. The constructed plasmid contains the target protein and a His_6 tag at the N terminus, which was confirmed by sequencing.

A total of seven mutants were generated: H17A, R18A, E44A, D46A, H59A, E119A, and K121A. Site-directed mutations were introduced using the specific primer couples to amplify the whole pETM-10 plasmid containing the wild-type ttGDPD gene. The mutated DNA sequences were entirely sequenced to confirm that only the appropriate mutations were incorporated into the nucleic acid.

Production of ttGDPD and mutants

The wild-type ttGDPD and mutants were expressed in *E. coli* Rosetta (DE3), except for the H17A mutant that could not be expressed. Proteins were purified by passage through a nickel-affinity column, and a further purification step was performed by size-exclusion chromatography using a Superdex 200 column (Amersham). The pure protein was kept in 5 m*M* Tris-HCl (pH 8.0) after concentration to 20 mg/mL.

Crystallization

The crystals of recombinant ttGDPD were grown at 20°C using the hanging-drop, vapor-diffusion method. Drops consisted of 1 μL of protein solution and 1 μL of mother liquor [0.1*M* Hepes (pH 7.5), 18 % PEG4000, 10 % iso-propanol, 0.05*M* $CaCl_2$] and glycerol was added to the protein solution to 2.5 % (v/v). Streak seeding was carried out after 2 days.[19] Crystals appeared within several hours, and crystals suitable for X-ray diffraction studies were obtained after several days growth.

Data collection and processing

Crystals in the mother liquor plus 10 % (v/v) 1,4-butanediol as a cryoprotectant were flash-frozen in liquid nitrogen The complete data were collected at a Rikagu R-axis IP IV++ detector, and were integrated and scaled with DENZO and SCALEPACK[20]; the statistics of data collection are summarized in Table I, and show that the crystal diffracted to beyond 2 Å resolution, and belongs

to space group $P2_1$. There are two molecules in an asymmetric unit.

Structure determination and refinement

A molecular replacement (MR) solution was found by PHASER in the CCP4 suite using data from a single crystal of ttGDPD,[21] using the glycerophosphodiester phosphodiesterase from *T. maritima* (PDB entry 1O1Z) as the search model, which displays 31% sequence identity with ttGDPD. The initial model was built by ARP/wARP,[22] and further refined in CNS[23]; the program COOT[24] was used for inspection and manual improvement of the model. The refinement results are summarized in Table I.

Glycerophosphodiester phosphodiesterase assay

After dialysis against Tris-HCl (pH 8.0), 50 μM EDTA, dialysis against six changes Tris-HCl (pH 8.0) was done to remove EDTA completely. The enzymatic activity of ttGDPD was examined at 25°C by measuring the production of glycerol 3-phosphate in a coupled spectrophotometric assay as described by Larson *et al.*[1] The 1 mL assay mixture contained 0.9 mL of 1*M* hydrazine hydrate in 1.5% glycine buffer (pH 9.0), 0.5 m*M* NAD, 10 m*M* $MgCl_2$, 10 U of glycerol-3-phosphate dehydrogenase/mL, and 0.5 m*M* glycerophosphorylcholine. The rate of NAD reduction was measured by recording the increase in absorbance at 340 nm.

RESULTS

Overall structure

Using the crystal structure of GDPD from *T. maritima* as the model, we have determined the 1.91 Å crystal structure of ttGDPD by the molecular replacement (MR) method. Two monomers form an asymmetric dimer that contains 482 of the expected 504 amino acid residues, shown in Figure 1(A). In the refined model, molecule A includes residues 11–249, but 10 residues of the N-terminus and three residues of the C terminus could not be modeled because of the lack of electron density. Molecule B comprises residues 10–252, but we could not model nine residues of the N-terminus. In addition, the loop (121–127) above the cleft at the C terminus of the barrel of ttGDPD has poor electron density, suggesting that this loop is flexible and could form the lid of active site. A total of 333 water molecules, two Ca atoms, and two glycerol molecules were included in the model.

The ttGDPD monomer exhibits a TIM-barrel fold and displays a central eight-stranded (β1, β2, β4, β5, β6, β7, β8, β9) parallel β-sheet barrel, which is surrounded by eight α-helices (α1, α3, α4, α5, α6, α7, α8, α9). A 3_{10} helix is inserted between strand β7 and helix α7. An additional domain (residues 47–101) is inserted in the second β sheet and the second α helix. This domain was first reported in 2004,[11] and was called the GDPD-insert (GDPD-I) domain, as a novel domain with a new fold. This domain consists almost entirely of loops subsequent to β2 and β3, besides two short 3_{10} helices and a four residue α-helix, see Figure 1(C). The structure of ttGDPD and GDPD from *T. maritima* (PDB entry 1o1z) can be superimposed with an r.m.s.d of 1.5Å for the C^{α} atoms. A comparison of these two structures shows an additional loop region (residues 85–97) in ttGDPD, in which there is a 3_{10} helix, see Figure 1(D); The loop between the β6 and α6 motif (loop 6) of ttGDPD, which is considerably different from 1o1z in main-chain conformation, plays some important roles in dimerization, see Figure 1(D).

Two monomers associate tightly to form the dimeric structure shown in Figure 1(B). The r.m.s.d between the two monomers is about 0.36 Å. The results of gel-filtration chromatography and native polyacrylamide gel electrophoresis show that ttGDPD is a dimer in solution, suggesting that the dimer could be the functional unit of ttGDPD. The loop between β6 and α6 (loop 6), described previously, has an important role in dimer formation. It can contact loop 6 and loop 5 (loop between β5 and α5) of the other monomer. The two Cys175 located in loop 6 of the A and the B chain produce an intermolecular disulfide bridge, and there are two hydrogen bonds between loop 6 and loop 5 of the neighbor molecule. So, the interaction between the two monomers is mediated by loop 6 and loop 5. In GDPDs, the sequence of loop 6 and Cys175 are not strictly conserved. Formation of the ttGDPD dimer involving an intermolecular disulfide bridge and hydrogen bonds is almost unique, with most GDPDs existing as the monomer.

Active site of ttGDPD

The full length of ttGDPD from *T. tengcongensis* is homologous to the GDPD of *A. tumefaciens* (PDB entry 1zcc), *T. maritima* (PDB entry 1o1z), *E. coli* (PDB entry 1vd6) sharing 31%, 34%, and 26% identical amino acid residues, respectively, as shown in Figure 2(A), and analysis by the program DALI[27] shows significant similarity, giving *Z* scores of 25, 26, and 27, respectively. The r.m.s.d between ttGDPD and these structures are 1.53 Å, 1.51 Å, and 1.46 Å, respectively. The very high level of sequence identity, and the topological and structural resemblance provide strong evidence that this molecule is a member of the glycerophosphodiester phosphodiesterase superfamily.

By superimposition of these structures, we identified a cluster of strictly conserved residues (His17, Arg18, Glu44, Asp46, His59, Glu119, and Lys121) around the cavity at the C terminus of the barrel of ttGDPD, and they form an electronegative cleft, as shown in

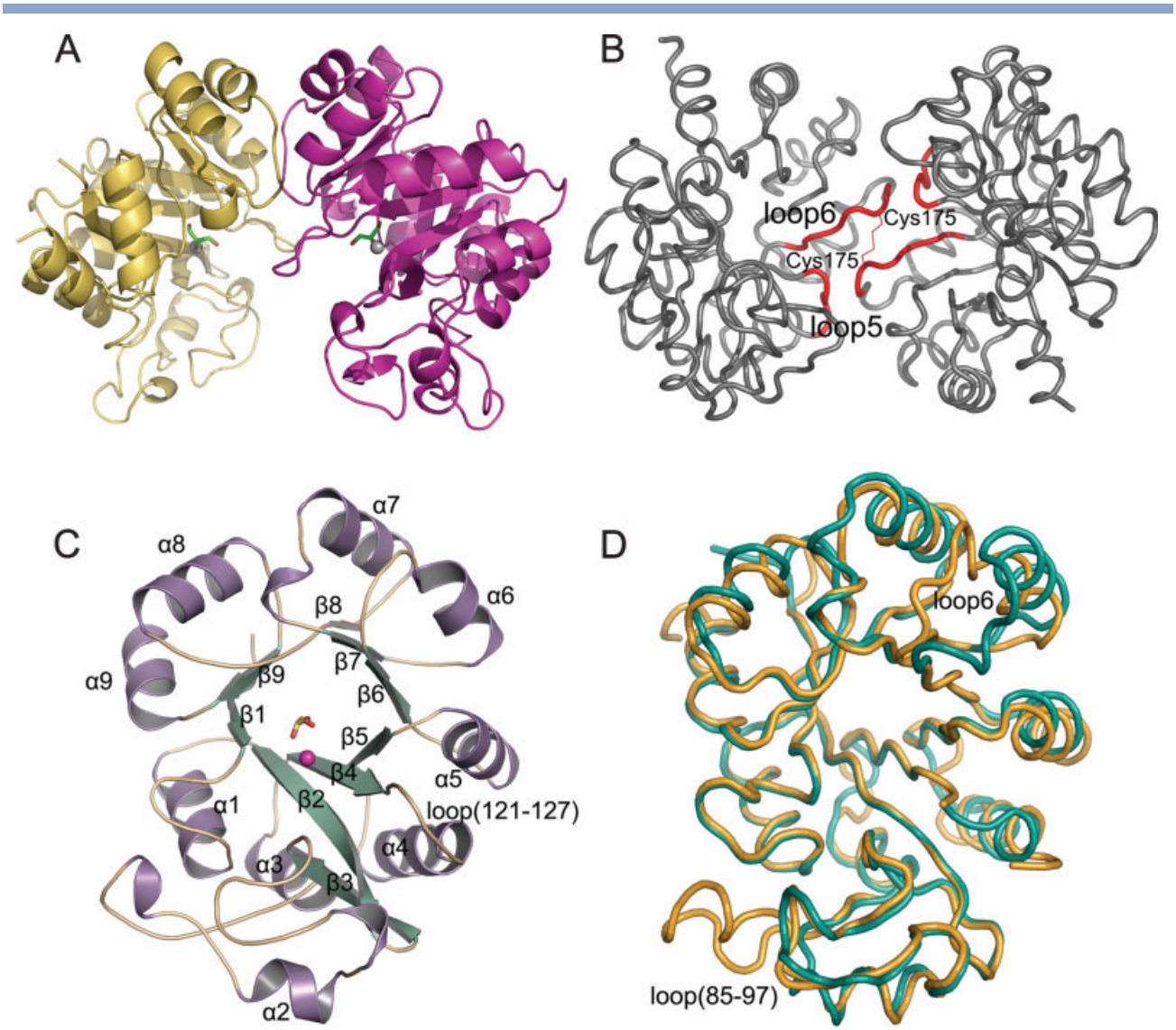

Figure 1

The structure of the ttGDPD dimer and monomer. ***A****: Ribbon representation of ttGDPD dimer with monomers shown in different colors. The Ca ion is shown in grey, and the glycerol is shown in stick mode in green.* ***B****: The overall fold of the ttGDPD dimer showing the distinct motif responsible for the dimerization. The motifs of monomers contacting each other are shown in red. The line mode bond within loop 6 represents the disulfide bridge between the two Cys residues located in loop 6 of molecules A and B.* ***C****: The monomer structure of ttGDPD. α-Helices, β-sheets, and loops are colored light purple, light green, and light yellow, respectively. The bound Ca ion is colored magenta and the glycerol molecule is shown in stick mode in yellow. The loop (121–127) appears to be flexible and may be the lid of the active cleft of ttGDPD.* ***D****: The monomer structure of ttGDPD (yellow) overlaid with the T. maritima GDPD monomer (cyan). Loop 6 and loop (85–97) of ttGDPD have marked differences between them.*

Figure 2(B), in which a Ca ion and a glycerol molecule are bound. This cleft at the C terminus of the barrel is considered to be the active region in the TIM-barrel superfamily.[28]

Glu44, Asp46, and Glu119 constitute a metal-binding site in that cleft of ttGDPD, with a Ca atom bound. Difference electron density maps show the presence of a 6σ electron density peak in the metal-binding site. We believe that this Ca atom was introduced by the $CaCl_2$ that was used during crystallization. We have solved the no metal-binding ttGDPD structure using a crystal formed in the absence of $CaCl_2$, and there is no density in that position. Other metal ions (Mg, Co, Zn, etc.) have been found in that site in several homologous structures of ttGDPD.

With a glycerol molecule binding at the Ca atom, Glu44, Asp46, Glu119, two water molecules and the OH2 group of glycerol compose a octahedral arrangement, showing tetragonal bipyramidal coordination. Glu119 and Wat363 become the axial ligands, with Asp46, Glu44,

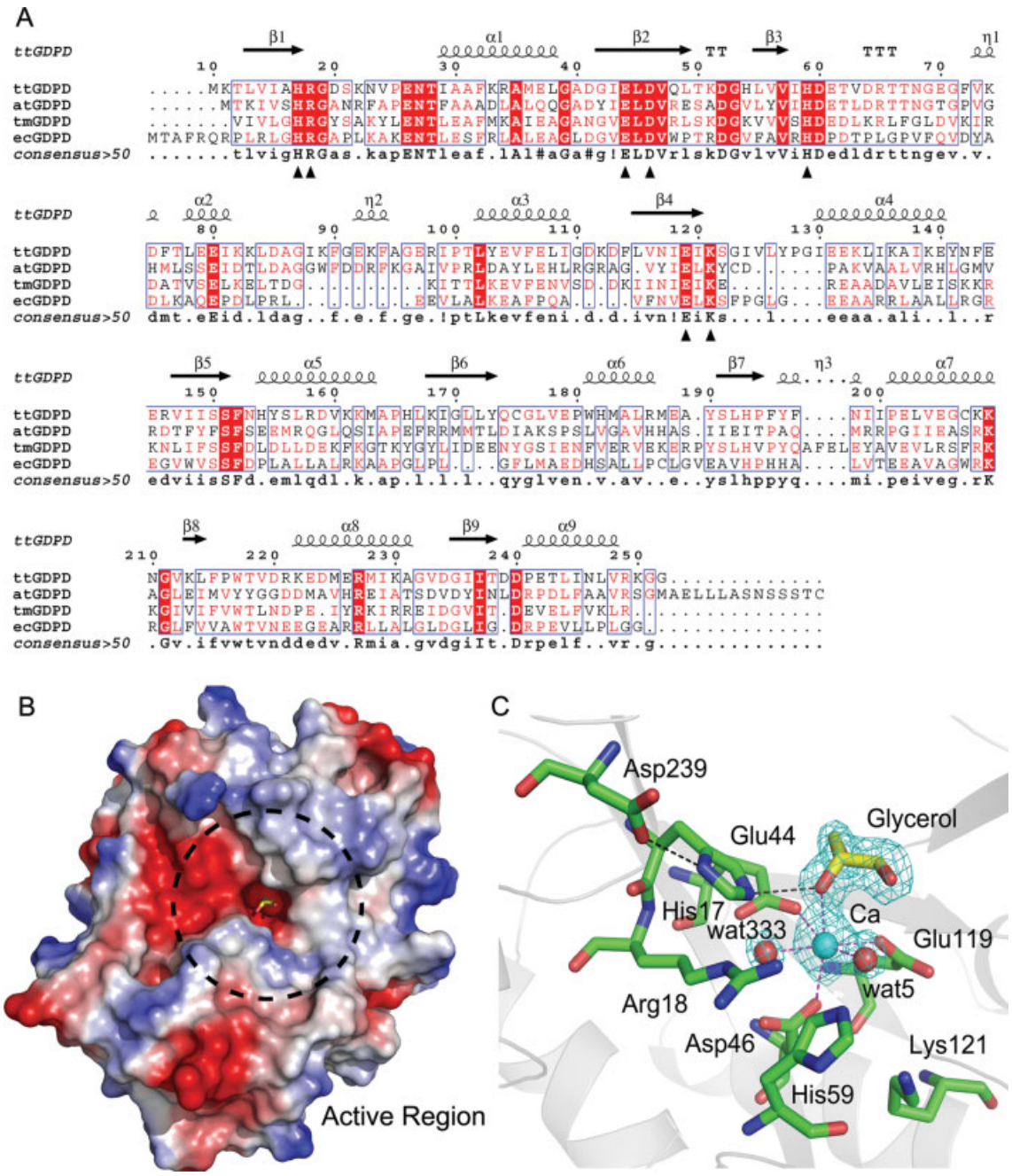

Figure 2

Alignment of ttGDPD among the homologous proteins available in the PDB and the active site architecture of ttGDPD. ***A****: Structure-based sequence alignment of some GDPDs available in the PDB. The sequence alignment was calculated with Multalin*[25] *and represented with Espript.*[26] *Secondary structures of ttGDPD are shown above the alignments. Triangles indicate strictly conserved residues investigated in this work using site-directed mutagenesis. ttGDPD, GDPD from T. tengcongensis (PDB entry 2pz0); atGDPD: GDPD from A. tumefaciens (PDB entry 1zcc); tmGDPD: GDPD from T. maritima (PDB entry 1o1z); ecGDPD: GDPD from E. coli (PDB entry 1vd6).* ***B****: The electrostatic potential surface map of ttGDPD. The electronegative cleft is the active region of ttGDPD (broken black line around it), where a Ca ion and a glycerol molecule are located.* ***C****: Active site structure of ttGDPD. The Ca ion is shown in cyan, and water molecules are shown in red. $2F_o$-F_c electron density of Ca ion, water and glycerol are contoured at 1.0σ. The broken purple lines represent the coordination bonds, and the broken black lines represent the hydrogen bonds. [Color figure can be viewed in the online issue, which is available at www.interscience.wiley.com.]*

Wat5, and the OH2 group of glycerol being in a plane. Glycerol is the polar moiety of the glycerophosphodiester substrates of GDPD. Glycerol can be found binding at a divalent metal ion in the structure of 1v8d and 1ydy. It is reasonable to deduce that this site is the active site of GDPD, and glycerol is a mimic of the true substrate.

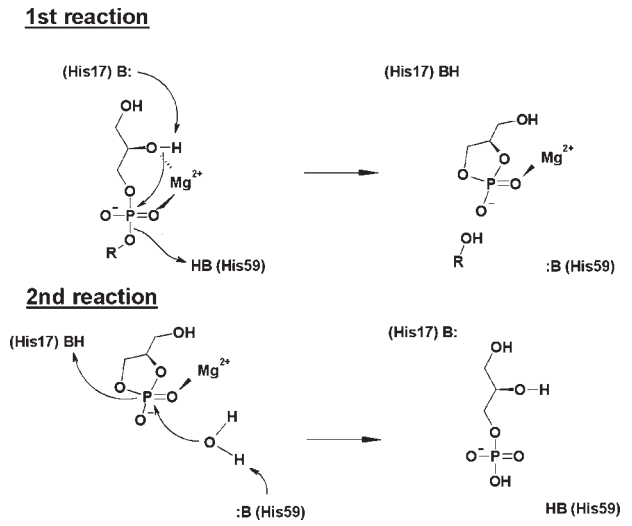

Figure 3
A diagram of a possible mechanism of ttGDPD.

This ttGDPD crystal structure represents the substrate-binding mode of GDPD.

Around the cleft of ttGDPD, His17 and His59 are strictly conserved. On the basis of the catalytic mechanism of PI-PLC,[17] these two His are the essential residues participating in the catalytic process. The NE2 atom of His17 and the OH2 group of glycerol form a hydrogen bond with a length of 2.8 Å. The carboxyl group of Asp239 forms a hydrogen bond with the ND1 atom of His17, which can stabilize the tautomeric state of the imidazole group of His17, see Figure 3. The other essential residue, His59, is too far away to contact the glycerol molecule directly.

Enzyme activity of the ttGDPD mutant

On the basis of the results of multisequence alignment and analyses of the active site of ttGDPD, a series of strictly conserved residues were assumed to take part in the ttGDPD catalytic mechanism. Seven strictly conserved residues were chosen as targets for site-directed mutagenesis to investigate the catalytic mechanism of ttGDPD. To identify the role of the metal ion in the catalytic process of ttGDPD, we constructed 3 mutants of the metal-binding residues (Glu44-Ala, Asp46-Ala, and Glu119-Ala); two mutants of the catalytic residues His17 and His59-Ala; two more mutants, Arg18-Ala and Lys121-Ala. The two residues surrounded by the glycerol molecule are strictly conserved, and may have important roles in the catalytic process of ttGDPD. Six of these mutants have been expressed in *E. coli*, and the enzyme activity of these mutants has been determined, see Table II. The three mutants of the metal-binding residues E44A, D46A, and E119A are completely inactive, indicating that ttGDPD is a metal ion-dependent enzyme. We constructed the plasmids of mutants H17A and H59A; the H59A mutant retains 1.39% activity but the H17A mutant cannot be expressed. On the basis of the catalytic mechanism of PI-PLC, we can consider two residues as the active residues of ttGDPD. Mutant R18A and K121A, with 10.7% and 4.7% activity, respectively, show that the two residues have an important influence on the catalytic activity of ttGDPD.

DISCUSSION

ttGDPD is a metal ion-dependent enzyme

As shown in Table II, ttGDPD has no enzymatic activity in the absence of divalent metal cations when treated with EDTA, and has a high level of activity in the presence of Mg2+ but a relatively low level of activity in the presence of Ca2+ (28.5%). It is clear that the activity of ttGDPD is dependent on a divalent metal cation. The former idea, that Mg^{2+} is an inhibitor of GDPD and GDPD is stimulated by Ca^{2+} is incorrect.[1]

In ttGDPD, the side chain oxygen atoms of E44, D46, and E119 coordinate to a Ca ion that is chelated by the OH2 group of a glycerol molecule, a mimic of the true substrate. We propose that ttGDPD binds the substrate via the coordination effect of the metal ion. We have measured the enzymatic activity of ttGDPD mutants E44A, D46A, and E119A, and have shown that the three mutants were completely inactive, confirming that these three metal-binding residues are essential for substrate binding. Future work trying to use isothermal titration calorimetry (ITC)[29] to measure the binding constant of substrate with ttGDPD in the presence and absence of bivalent ion will further support our conclusion that ttGDPD is a metal ion-dependent enzyme.

Table II
Enzyme Activity Assay of Wild-Type-ttGDPD With Different Metal Ions and Enzyme Activity of ttGDPD Mutants with 10 mM $MgCl_2$

	Activity (%)
wt-ttGDPD	
+10 m*M* $MgCl_2$	100 ± 2.25
+10 m*M* $CaCl_2$	28.5 ± 0.37
No metal	0
ttGDPD mutant	
E44A	0
D46A	0
E119A	0
H59A	1.39 ± 0.27
R18A	10.7 ± 0.26
K121A	4.7 ± 0.15

For assay methods, see Materials and Methods. The activity of wild-type GDPD with $MgCl_2$ was taken as 100%. (±S.E. represents the standard error based on measurements of at least three independent assays).

The possible catalytic mechanism of ttGDPD

In CATH,[30,31] GDPD has been classed as a member of the superfamily of phosphatidylinositol (PI) phosphodiesterases. In this family, PI-PLC (the phosphatidylinositol-specific phospholipase C) from *Bacillus cereus* has a low level of primary sequence identity with ttGDPD (<20%) and poor similarity of the general structure, although both are TIM-barrel folds and belong to the phospholipases C. The superposition of these two structures shows an overlap of the catalytic residues His32 and His82 of PI-PLC with His17 and His59 of ttGDPD. In PI-PLC, His32 and His82 have the role of general acid and general base in catalyzing the hydrolysis of the 3′-5′ phosphodiester bond.[17,32] His17 and His59 of ttGDPD have the same position and orientation as the corresponding residues His32 and His82 in PI-PLC. Furthermore, ttGDPD and PI-PLC hydrolyze identical bonds in different substrates. We can infer that the catalytic mechanism of ttGDPD is similar to that of PI-PLC, as a mechanism of general base and acid catalysis with His17 and His59 of ttGDPD.

We verified the role of His17 and His59 of ttGDPD in the catalysis by site-directed mutagenesis. The H59A mutant has a very low level of activity and the H17A mutant cannot be expressed, but this strictly conserved histidine residue has a critical role in a series of homologues.[17,33] For ttGDPD, Mg ion is a much stronger activator of this enzyme than Ca ion, although Ca ion is also capable to activate it in a minor degree. The catalytic mechanism proposed for ttGDPD on the basis of an acid–base reaction is illustrated by Figure 3. This mechanism is a two-step reaction; moreover, the glycerol moiety and the phosphate moiety form a cyclic phosphate intermediate. In the first reaction, His17 acts as a general base, accepting a proton from the OH2 group of the glycerol moiety of glycerophosphodiester, and leads to an in-line attack on the phosphorus. At the same time, His59 acts as a general acid, and donates a proton to the oxygen of the leaving group (R—OH). A possible role for the metal in this reaction would be acting as an electrophile to stabilize the intermediate. In the second reaction, the catalytic roles of His17 and His59 are reversed. His59 deprotonates a nearby water molecule, which initiates a nucleophilic attack on the phosphorus of the cyclic phosphate, and His17 now acts as a general acid donates a proton and forms the final product.

Simulation of the true substrate binding in the enzyme

The glycerol molecule in ttGDPD mimics the glycerol moiety of glycerophosphodiester, which is the stubstrate of the enzyme *in vivo*. The phosphate moiety of glycerophosphodiester may also bind with the enzyme, and it cannot be represented by the structure of ttGDPD. In the structure of GDPD from *A. tumefaciens* (PDB entry 1zcc),[12] a sulfate molecule binds in proximity to the active site. Superposition of the active site of ttGDPD and 1zcc shows that the sulfate ion in 1zcc is located outside of the OH3 group of the glycerol molecule in ttGDPD, see Figure 4. The sulfate ion can be considered to represent the phosphate moiety of the substrate, and the structure of 1zcc can imply the binding mode of the phosphate moiety and GDPD. In 1zcc, the sulfate molecule is linked to His7 and Arg8, which correspond to His17 and Arg18 of ttGDPD, with hydrogen bonds, suggesting that the phosphate moiety of substrate can contact these two residues in ttGDPD. And His17 is the catalytic residue of ttGDPD. Measurement of the activity of mutant of R18A shows that only 10.7% of activity remained, suggesting that Arg18 is not the key residue for the catalytic activity of ttGDPD, but it may stabilize the orientation of the phosphate moiety of the substrate and improve the efficiency of catalysis.

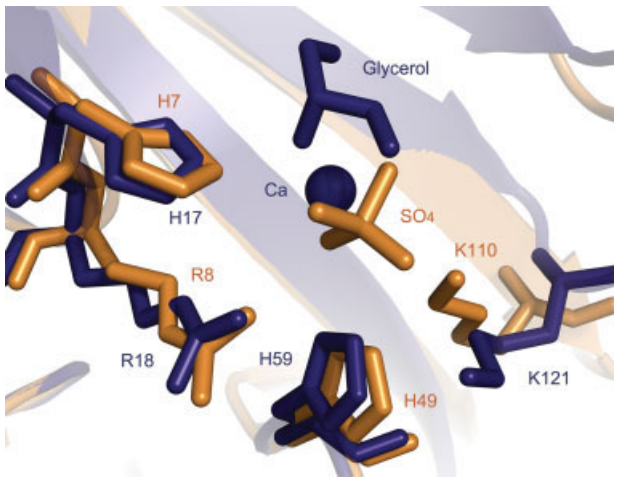

Figure 4

Superimposition of the active sites of ttGDPD and 1zcc. ttGDPD is shown in purple and 1zcc is shown in yellow. The bound sulfate ion in 1zcc is located just outside the OH3 group of the glycerol molecule in ttGDPD, and it may well infer the binding mode of the phosphate moiety of the substrate of ttGDPD. In 1zcc, Lys110 is closer to the active site than the corresponding Lys121 of ttGDPD and it is proposed to contribute to the electronic interaction between the lysine residue and the sulfate ion. [Color figure can be viewed in the online issue, which is available at www.interscience.wiley.com.]

Figure 4 shows that the sulfate molecule is very close to the metal-binding site in 1zcc. It can be suggested that when ttGDPD binds the true substrate, the phosphate moiety forms more coordination bonds to the metal ion, bringing the phosphate moiety close to the OH2 group of the glycerol moiety facilitating the nucleophilic attack of the phosphorus atom by 2-O^-. In 1zcc, the positively charged amino group of Lys110 is about 3.9 Å away from the negatively charged sulfate molecule, allowing some electronic interaction between them. This lysine residue is strictly conserved in GDPDs; moreover, the

enzymatic activity of mutant K121A of ttGDPD is sharply reduced (only 4.7% remained). All these facts together suggest that this lysine residue influences the catalysis of GDPD via electronic interaction with the phosphate moiety of the substrate. In 1zcc, Lys110 is closer to the active site than it is in ttGDPD, and it may contribute to the electronic interaction of the sulfate ion. So, we can predict that the phosphate moiety of the substrate can cause Lys121 of ttGDPD to move when it binds glycerophosphodiester, the true substrate. Furthermore, in ttGDPD, Lys121 is the first residue of loop (121–127), which is located above the active site cleft and is disordered in the structure considered as the upper lip of that cleft. When ttGDPD binds to the substrate, Lysine121 can interact with the substrate to pull the loop tight, and thus close the active cleft.

CONCLUSION

We have solved the crystal structure of ttGDPD with a Ca ion and the substrate mimic glycerol bound. We have identified ttGDPD as a metal ion-dependent enzyme and shown that the metal ion has an essential role in the enzyme activity via coordinating with the substrate. We have described a possible catalytic mechanism for ttGDPD with His17 and His59 as general acid and base. We have shown that some other strictly conserved residues around the active site can have important roles. The high level of sequence identity of GDPDs suggests the features and catalytic mechanism of ttGDPD can be applicable to other members of this superfamily.

ACKNOWLEDGMENTS

We thank Prof. Run-Sheng Chen for providing the *T. tengcongensis* strains. We also thank the staff of the Institute of Biophysics, Yi Han in charge of X-ray radiation facility. We thank Dr. Zai-Rong Zhang for assistance in enzyme activity assay and useful discussion. Also, we thank EMBL for providing pETM-10 vector.

REFERENCES

1. Larson TJ, Ehrmann M, Boos W. Periplasmic glycerophosphodiester phosphodiesterase of *Escherichia coli*, a new enzyme of the glp regulon. J Biol Chem 1983;258:5428–5432.
2. Tommassen J, Eiglmeier K, Cole ST, Overduin P, Larson TJ, Boos W. Characterization of two genes, glpQ and ugpQ, encoding glycerophosphoryl diester phosphodiesterases of *Escherichia coli*. Mol Gen Genet 1991;226(1/2):321–327.
3. Fisher E, Almaguer C, Holic R, Griac P, Patton-Vogt J. Glycerophosphocholine-dependent growth requires Gde1p (YPL110c) and Git1p in *Saccharomyces cerevisiae*. J Biol Chem 2005;280:36110–36117.
4. van der Rest B, Boisson AM, Gout E, Bligny R, Douce R. Glycerophosphocholine metabolism in higher plant cells. Evidence of a new glyceryl-phosphodiester phosphodiesterase. Plant Physiol 2002;130:244–255.
5. Zheng B, Berrie CP, Corda D, Farquhar MG. GDE1/MIR16 is a glycerophosphoinositol phosphodiesterase regulated by stimulation of G protein-coupled receptors. Proc Natl Acad Sci USA 2003;100:1745–1750.
6. Schwan TG, Battisti JM, Porcella SF, Raffel SJ, Schrumpf ME, Fischer ER, Carroll JA, Stewart PE, Rosa P, Somerville GA. Glycerol-3-phosphate acquisition in spirochetes: distribution and biological activity of glycerophosphodiester phosphodiesterase (GlpQ) among *Borrelia* species. J Bacteriol 2003;185:1346–1356.
7. Lin EC. Glycerol dissimilation and its regulation in bacteria. Annu Rev Microbiol 1976;30:535–578.
8. Fan X, Goldfine H, Lysenko E, Weiser JN. The transfer of choline from the host to the bacterial cell surface requires glpQ in *Haemophilus influenzae*. Mol Microbiol 2001;41:1029–1036.
9. Yanaka N, Nogusa Y, Fujioka Y, Yamashita Y, Kato N. Involvement of membrane protein GDE2 in retinoic acid-induced neurite formation in Neuro2A cells. FEBS Lett 2007;581:712–718.
10. Rao M, Sockanathan S. Transmembrane protein GDE2 induces motor neuron differentiation in vivo. Science 2005;309:2212–2215.
11. Santelli E, Schwarzenbacher R, McMullan D, Biorac T, Brinen LS, Canaves JM, Cambell J, Dai X, Deacon AM, Elsliger MA, Eshagi S, Floyd R, Godzik A, Grittini C, Grzechnik SK, Jaroszewski L, Karlak C, Klock HE, Koesema E, Kovarik JS, Kreusch A, Kuhn P, Lesley SA, McPhillips TM, Miller MD, Morse A, Moy K, Ouyang J, Page R, Quijano K, Rezezadeh F, Robb A, Sims E, Spraggon G, Stevens RC, van den Bedem H, Velasquez J, Vincent J, von Delft F, Wang X, West B, Wolf G, Xu Q, Hodgson KO, Wooley J, Wilson IA. Crystal structure of a glycerophosphodiester phosphodiesterase (GDPD) from *Thermotoga maritima* (TM1621) at 1.60 A resolution. Proteins 2004;56:167–170.
12. Rao KN, Bonanno JB, Burley SK, Swaminathan S. Crystal structure of glycerophosphodiester phosphodiesterase from *Agrobacterium tumefaciens* by SAD with a large asymmetric unit. Proteins 2006;65:514–518.
13. Jackson CJ, Carr PD, Liu JW, Watt SJ, Beck JL, Ollis DL. The structure and function of a novel glycerophosphodiesterase from *Enterobacter aerogenes*. J Mol Biol 2007;367:1047–1062.
14. Jackson CJ, Carr PD, Kim HK, Liu JW, Ollis DL. The purification, crystallization and preliminary diffraction of a glycerophosphodiesterase from *Enterobacter aerogenes*. Acta Crystallogr 2006;62(Part 7):659–661.
15. Bachmann AS, Duennebier FF, Mocz G. Genomic organization, characterization, and molecular 3D model of GDE1, a novel mammalian glycerophosphoinositol phosphodiesterase. Gene 2006;371:144–153.
16. Xue Y, Xu Y, Liu Y, Ma Y, Zhou P. *Thermoanaerobacter tengcongensis* sp. nov., a novel anaerobic, saccharolytic, thermophilic bacterium isolated from a hot spring in Tengcong, China. Int J Syst Evol Microbiol 2001;51(Part 4):1335–1341.
17. Heinz DW, Ryan M, Bullock TL, Griffith OH. Crystal structure of the phosphatidylinositol-specific phospholipase C from *Bacillus cereus* in complex with myo-inositol. EMBO J 1995;14:3855–3863.
18. Bao Q, Tian Y, Li W, Xu Z, Xuan Z, Hu S, Dong W, Yang J, Chen Y, Xue Y, Xu Y, Lai X, Huang L, Dong X, Ma Y, Ling L, Tan H, Chen R, Wang J, Yu J, Yang H. A complete sequence of the *T. tengcongensis* genome. Genome Res 2002;12:689–700.
19. Zhu DY, Zhu YQ, Xiang Y, Wang DC. Optimizing protein crystal growth through dynamic seeding. Acta Crystallogr 2005;61(Part 6):772–775.
20. Otwinowski Z, Minor W. Processing of X-ray diffraction data collected in oscillation mode. Methods Enzymol 1997;276:307–326.
21. Storoni LC, McCoy AJ, Read RJ. Likelihood-enhanced fast rotation functions. Acta Crystallogr 2004;60(Part 3):432–438.
22. Lamzin VS, Wilson KS. Automated refinement of protein models. Acta Crystallogr 1993;49(Part 1):129–147.
23. Brunger AT, Adams PD, Clore GM, DeLano WL, Gros P, Grosse-Kunstleve RW, Jiang JS, Kuszewski J, Nilges M, Pannu NS, Read RJ, Rice LM, Simonson T, Warren GL. Crystallography & NMR system: a new software suite for macromolecular structure determination. Acta Crystallogr 1998;54(Part 5):905–921.

24. Emsley P, Cowtan K. Coot: model-building tools for molecular graphics. Acta Crystallogr 2004;60(Part 12 Part 1):2126–2132.
25. Corpet F. Multiple sequence alignment with hierarchical clustering. Nucleic Acids Res 1988;16:10881–10890.
26. Gouet P, Courcelle E, Stuart DI, Metoz F. ESPript: analysis of multiple sequence alignments in PostScript. Bioinformatics (Oxford, England) 1999;15:305–308.
27. Holm L, Sander C. Protein structure comparison by alignment of distance matrices. J Mol Biol 1993;233:123–138.
28. Nagano N, Orengo CA, Thornton JM. One fold with many functions: the evolutionary relationships between TIM barrel families based on their sequences, structures and functions. J Mol Biol 2002; 321:741–765.
29. Ababou A, Ladbury JE. Survey of the year 2004: literature on applications of isothermal titration calorimetry. J Mol Recognit 2006;19: 79–89.
30. Orengo CA, Bray JE, Buchan DW, Harrison A, Lee D, Pearl FM, Sillitoe I, Todd AE, Thornton JM. The CATH protein family database: a resource for structural and functional annotation of genomes. Proteomics 2002;2:11–21.
31. Pearl FM, Lee D, Bray JE, Buchan DW, Shepherd AJ, Orengo CA. The CATH extended protein-family database: providing structural annotations for genome sequences. Protein Sci 2002;11: 233–244.
32. Heinz DW, Ryan M, Smith MP, Weaver LH, Keana JF, Griffith OH. Crystal structure of phosphatidylinositol-specific phospholipase C from *Bacillus cereus* in complex with glucosaminyl(α 1→6)-D-myo-inositol, an essential fragment of GPI anchors. Biochemistry 1996;35:9496–9504.
33. Murakami MT, Fernandes-Pedrosa MF, Tambourgi DV, Arni RK. Structural basis for metal ion coordination and the catalytic mechanism of sphingomyelinases D. J Biol Chem 2005;280:13658–13664.